ELSEVIER

Carbohydrate Research 280 (1996) 85–99

CARBOHYDRATE RESEARCH

Degradation of double-stranded xanthan by hydrogen peroxide in the presence of ferrous ions: comparison to acid hydrolysis

Bjørn E. Christensen *, Mildrid H. Myhr, Olav Smidsrød

Norwegian Biopolymer Laboratory, Department of Biotechnology, University of Trondheim, NTH, N-7034 Trondheim, Norway

Received 4 April 1995; accepted in revised form 1 August 1995

Abstract

Conformationally ordered, double-stranded xanthan, degraded in the presence of H_2O_2 and Fe^{2+} (at 20°C) or in dilute acid (0.1 M HCl at 80°C), produced xanthan variants with weight-average molecular weights (M_w) ranging from 2×10^6 to 5.4×10^4. In both cases the fraction of cleaved linkages in the glucan backbone (α), measured as reducing ends, increased to very high values (0.05 for $M_w = 2\text{–}3 \times 10^4$), demonstrating that a large number of linkages in the backbone could be cleaved without a correspondingly large reduction in M_w, in accordance with the double-stranded nature of xanthan. Extensive degradation (more than 10-fold reduction in M_w) in both cases released single-stranded, conformationally disordered oligomers; this release was accompanied by an increase in the rate of acid hydrolysis of the glucan backbone and a pronounced increase in the rate of release of glucose monomer. In contrast, there was no significant change in the rate of reducing end-group formation associated with the release of oligomers upon degradation with H_2O_2/Fe^{2+}. Both types of degradation were accompanied by changes in the composition of the side chains. However, in contrast to acid hydrolysis, where the terminal β-D-mannose is preferentially hydrolyzed, the reaction with H_2O_2/Fe^{2+} resulted in removal of both mannose and glucuronic acid at approximately equal rates. This observation can be explained by a preferential attack on the inner α-D-mannose, with concomitant removal of the entire side chain. Removal of side chains and the release of single-stranded oligomers by H_2O_2/Fe^{2+} strongly influenced the optical rotation and also broadened the chiroptically detected conformational transition, whereas no change in the transition temperature was observed.

Keywords: Xanthan; Degradation; Acid hydrolysis

* Corresponding author.

SSDI 0008-6215(95)00289-8

1. Introduction

Polysaccharides, including xanthan (Fig. 1), are susceptible to free-radical induced degradation, as in the presence of reducing agents and molecular oxygen. Such reactions are commonly referred to as oxidative–reductive depolymerizations (ORD) and result in cleavage of linkages in the polymeric backbone [1]. In comparison with many other water-soluble polymers, xanthan appears to be much more stable towards degradation, usually observed as loss of viscosity, as long as it exists in the double-stranded, ordered conformation. This is utilized in the oil industry, as in polymer flooding, and good performance has been obtained with the use of xanthan for extended periods [2]. When the degree of conformational order is decreased, as by lowering the ionic strength, the depolymerization proceeds much faster [3,4].

In previous articles we have explored in detail the behavior of double-stranded xanthan when exposed to random degradation, both theoretically [5] and experimentally through degradation by acid hydrolysis [3–8], and to a certain extent, by ORD [4]. Despite the changes occurring in the side chains, it was found that the double-stranded structure is quite robust, and persists until the glucan backbone finally becomes extensively depolymerized. The kinetics of the decrease of the weight-average molecular weight M_w also deviated strongly from that expected for random degradation of single-stranded polymers, since the apparent depolymerization rate was low in the initial stages of the degradation, but increased strongly with time [3–7]. This has been qualitatively attributed [5,7] to the double-stranded nature of xanthan. In the initial phase of the degradation, the non-covalent forces which cooperatively stabilize the double-stranded structure largely reduce the extent of strand separation although linkages in the

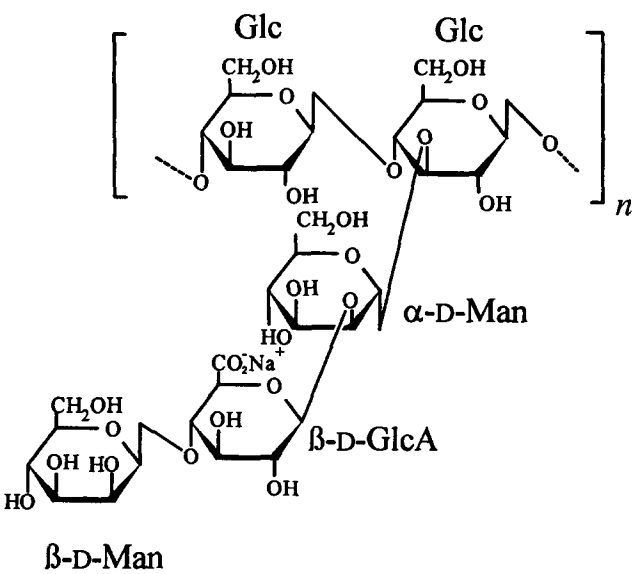

Fig. 1. Pentasaccharide repeating-unit corresponding to acetate- and pyruvate-free xanthan.

glucan backbone indeed are cleaved. A total break in the double-stranded structure will only occur when both strands are cleaved within a critical distance (h), which correspond to the minimum overlap distance needed for two single chains to form a duplex. The probability (q) for a total break to occur is given by eq (1) [9]:

$$q = (2h + 1)\alpha^2 \quad (1)$$

where α is the frequency or probability of (random) cleavage of any glycosidic linkage in the glucan backbone. So far, the relationship between q and α has not been experimentally determined for multiple-stranded polysaccharides, and analysis of α through analysis of reducing ends is therefore attempted here, both for acid hydrolysis and for degradation with H_2O_2/Fe^{2+}.

A second characteristic feature associated with the depolymerization of multiple-stranded polymers such as xanthan is the release of single-stranded, conformationally disordered fragments. They are formed when two scissions occur within the same chain, and within a distance along the chain (l) which is too short to allow the cooperative incorporation of the fragment in a multiple-stranded structure [5,7], namely when $l < h$. For acid hydrolysis of xanthan, such fragments have been identified by size-exclusion chromatography (SEC) or gel filtration [7,10], and it was further confirmed that they were indeed conformationally disordered. There was on the other hand no difference in the chemical composition, i.e., in the composition of the side chains, between the fragments and the parent double-stranded structures from which they were released [7]. These fragments, as well as the newly formed single-stranded regions of the adjacent chain, seem to be more rapidly degraded, resulting in the overall increase in the degradation rate (reduction in M_w) which is observed after extensive degradation [7].

Acid hydrolysis of xanthan leads to preferential hydrolysis of the terminal β-D-mannose in the side chains. This is attributed [3] to intramolecular catalysis by the carboxyl group of the adjacent glucuronic acid. In line with this it has been found that in acetan (xylinan), a polysaccharide structurally related to xanthan except that the terminal mannose is replaced by the trisaccharide α-L-Rha*p*-(1 → 6)-β-D-Glc*p*-(1 → 6)-α-D-Glc*p*-(1 → 4)-, the trisaccharide was preferentially released [8].

Compared to acid hydrolysis, ORD reactions are considered to be less specific, and the mechanisms which eventually result in cleavage of glycosidic bonds seem to be poorly understood. Simple copolymers like hyaluronate give rise to several types of end groups when degraded by ORD [11], but long single-stranded polymers are generally degraded in a random fashion [1,4,12]. In the case of xanthan it has been shown that the ratio between mannose and glucose decreases with time when degraded by ORD [13,14], showing that the side chains are affected in addition to the observed reduction in chain length [14] due to cleavage of linkages in the backbone. Moreover, the content of acetate and pyruvate also decreases [13–15].

In this work we explore in more detail the degradation of xanthan in the presence of H_2O_2 and Fe^{2+} (Fenton reagent), which is considered as an appropriate model for most ORD reactions occurring in nature or in technical applications. Both changes in the structure of the side chains, changes in M_w, and molecular-weight distributions are monitored, and the results are compared to those obtained for acid hydrolysis. Analysis of the formation of reducing ends in the glucan backbone is attempted, since this may

yield information about the degree of chain cleavage (α), which due to the double-stranded structure may be substantially higher than the apparent depolymerization rate calculated from the reduction of M_w [5,7].

Pyruvate- and acetate-free xanthan is used in the present study since a high and possibly varying level in the content of these substituents in the course of the degradation might influence the order–disorder transition, that is, both the transition temperature (T_m) and the width of the transition.

2. Experimental

Materials.—Xanthan containing one *O*-acetate and one pyruvate substituent per repeating unit [16] was obtained as a fermentation broth from Statoil A/S, Stavanger, Norway; 100 g of broth containing ~ 4 g/L of xanthan was diluted with 4 L of 10 mM NaCl, stirred for 12 h, and centrifuged (13,000 rpm, 30 min) to remove suspended particles. The supernatant was filtered through a 0.8-μm filter, and concentrated on a rotavapor to ~ 1 liter. The xanthan was precipitated with 2-propanol three times, redissolved in pure water, and freeze-dried. Pyruvate was removed by mild acid hydrolysis (0.1 M HCl, 3 h, 80°C) and acetate was removed by alkaline hydrolysis (0.025 M NaOH, 3 h, 20°C, N_2 atmosphere) [3,17–19]. The samples were subsequently dialyzed extensively against the buffer used in the degradation experiments.

Degradation.—Degradations with H_2O_2/Fe^{2+} were performed at 20 and 100°C using the pyruvate- and acetate-free xanthan (1.0 mg/mL) dissolved in a buffer containing 10 mM sodium acetate, 10 mM Na_2EDTA (pH 5.0). All glassware was acid-washed to remove traces of transition metal ions, which otherwise would lead to decreased reproducibility due to the strong dependence of metal ions on the rate of the ORD reaction [12]. The reaction was initiated by adding H_2O_2 (50 mM) and $FeCl_2$ (1.0 μM), and stopped by adding a mixture [20] of Na_2SO_3 (260 mM), thiourea (130 mM), and 2-propanol (26%). The values refer to final concentrations. It was shown in separate degradation experiments using a solution of *O*-(hydroxyethyl)cellulose that no further degradation, measured as reduction in viscosity, took place after addition of the mixture. About one third of each of the degraded samples was dialyzed (see below) extensively against 10 mM NaCl and analyzed by SEC–LALLS as described below. The rest was dialyzed against pure water and a major portion was subsequently freeze-dried.

Degradation of xanthan in 0.1 M HCl was performed as previously described [5], using the 2-propanol-precipitated sample described above. In this case the initial reduction in the content of pyruvate and acetate was omitted since the acid hydrolysis rapidly removes these substituents [3,7].

Dialyses.—All dialyses were performed using dialysis tubing (Visking, size 1-8/32 in.) obtained from Medicell International Ltd. The effective porosity was investigated by dialysing a series of cellooligosaccharides (DP 1 to 5), maltooligosaccharides (DP 1 to 7), and neocarratetraose, all obtained from Sigma. All of these oligosaccharides were found to be 100% dialyzable provided that enough time was allowed to reach equilibrium (typically 8–24 h at 4°C). Since M_w of the depolymerized xanthans is larger than

40,000, the dialyzable fraction consists primarily of fragments resulting from the release or degradation of side chains (DP 1 to 3), which are 100% dialyzable.

Analyses.—The chemical composition of partially degraded xanthans was determined by GLC following methanolysis and trimethylsilylation [3,7]. Molecular weights and molecular-weight distributions were determined by size-exclusion chromatography (SEC) combined with low-angle-laser light-scattering (LALLS) measurements (on-line) as previously described [7]. Reducing ends were analyzed by the Nelson reagent method [21]. Free glucose was analyzed using a commercial kit (Boeringer Mannheim; catalogue no. 716 251). The content of pyruvate and acetate was determined by ^{1}H-NMR spectroscopy [16,17,19].

3. Results

Reduction in M_w.—The decrease in M_w accompanying the degradation of double-stranded xanthan with H_2O_2/Fe^{2+} (20°C) and 0.1 M HCl (80°C) was analyzed by SEC–LALLS. The results are shown in Fig. 2. In both cases M_w is reduced from $\sim 2\text{–}3 \times 10^6$ to $\sim 5\text{–}10 \times 10^4$.

Formation of reducing ends in the glucan backbone.—Fig. 3 shows the fraction of detectable reducing end-groups formed in the two different degradations. It should be noted that measurements were performed on thoroughly dialyzed samples, thereby avoiding contributions from oligomers originating from the side-chains as well as from glucose monomer released from the backbone (see below). The results are expressed as the number of reducing ends formed relative to the total number of glucose residues. This ratio corresponds to the degree of chain scission (α), provided that a reducing end

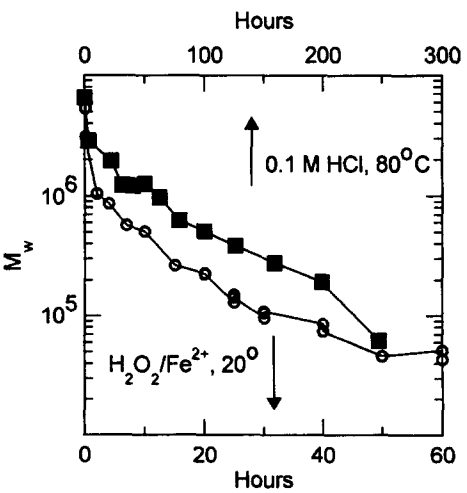

Fig. 2. Change in M_w following degradation of double-stranded xanthan in 50 mM H_2O_2 containing 1 μM $FeCl_2$, 20°C (○) and 0.1 M HCl, 80°C (■).

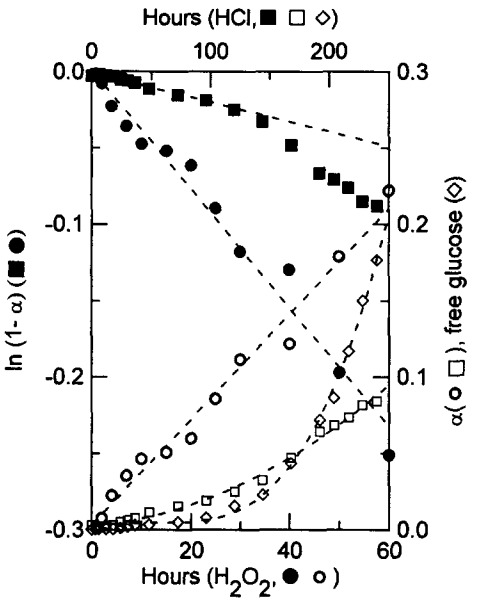

Fig. 3. Fraction of backbone (glucose) residues that appear as reducing ends (α) or as free monomers upon degradation with H_2O_2/Fe^{2+} at 20°C (α only) and 0.1 M HCl, 80°C. Symbols: For degradation with H_2O_2/Fe^{2+}: α (○) and $\ln(1-\alpha)$ (●). For degradation in 0.1 M HCl: α (□), $\ln(1-\alpha)$ (■) and fraction of glucose released as monomer (◇).

is formed each time a chain is cleaved. For degradation with H_2O_2/Fe^{2+}, α appears to increase linearly (within experimental error) with time to a value close to 0.22 obtained after 60 h. The plot of $\ln(1-\alpha)$ vs. time is also linear, indicating that the degradation obeys first-order kinetics. From this plot the rate of end group formation was found to be 0.0039 h^{-1}. An important observation is that the rate constant was independent of the degree of chain scission or consequently, independent of M_w.

A different behavior was observed with acid hydrolysis. Initially (0–120 h), a linear plot of $\ln(1-\alpha)$ versus time was obtained, with a calculated first order rate constant of 0.00019 h^{-1}. After this point the degradation became more rapid, with an estimated rate constant of ~ 0.0006 h^{-1}.

Release of glucose monomer.—Since the backbone of xanthan consists of glucose residues only, whereas the side chains are devoid of glucose, analysis of the changes in the amount of free glucose monomer may provide further information about the depolymerization process. For a truly random type of depolymerization, the fraction of glucose residues released as monomer should correspond to α^2 (the rate of destruction of free glucose is assumed to be negligible under the conditions used). The experimental data obtained with acid hydrolysis are included in Fig. 3. The analyses were in this case performed on undialyzed samples. In the early phase (0–50 h), free glucose is hardly detectable, in accordance with the low values of α in the same interval. However, after ~ 100 h the level increases rapidly and more pronounced than the amount of reducing ends. After 250 h, $\sim 20\%$ of the glucose originally present as polymer is released as

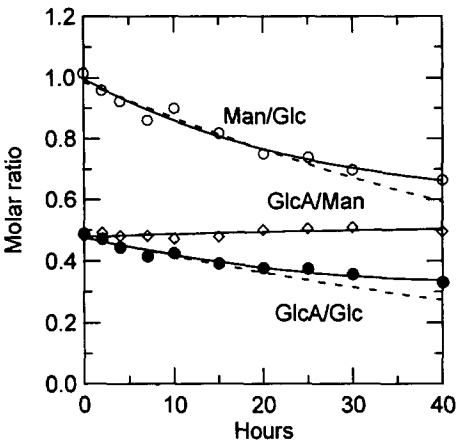

Fig. 4. Change in the molar ratios between mannose and glucose (○), glucuronic acid, and glucose (●) and between glucuronic acid and mannose (◇) upon degradation of xanthan with H_2O_2/Fe^{2+} at 20°C. Dotted lines correspond to a pseudo first-order process fitted to the data in the interval 0–15 h.

monomer. This is far more than the theoretical amount (α^2), which in this case should be 0.01 ($\alpha = 0.1$).

Chemical composition.—Fig. 4 shows the changes in molar ratios between mannose (Man) and glucose (Glc), and between glucuronic acid (GlcA) and glucose, resulting from degradation of xanthan with H_2O_2/Fe^{2+} at 20°C. The figure shows that Man/Glc is reduced from 1.0 to ~0.65, whereas GlcA/Glc is reduced from 0.5 to ~0.33. In contrast, the calculated ratio GlcA/Man is nearly constant or slightly increased. These changes can be explained by a mechanism which preferentially leads to cleavage of the linkage between the inner α-D-mannose and the glucan backbone, with a concomitant loss of the entire side chain. As shown in Fig. 4, a pseudo first-order rate constant of 0.015 h^{-1} (with respect to the α-D-mannose) describes the data fairly well up to about 15 h (dotted lines in Fig. 4). After this time the rate of the reaction seems to decrease slightly. For acid hydrolysis, rate constants have been determined earlier [7].

A degradation experiment was performed with H_2O_2/Fe^{2+} at 100°C, where xanthan is in the disordered conformation. In this case, the reaction was extremely rapid, and after 7.5 min the sample was degraded to a composition corresponding to sample degraded at 20°C for 40 h. After 7.5 min no change in the chemical composition was observed, indicating that most of the H_2O_2 had been consumed.

Molecular-weight distributions.—The molecular weight distributions obtained following degradation with H_2O_2/Fe^{2+} were analyzed at ambient temperature by size-exclusion chromatography (columns TSK G6000PWXL + G5000PWXL, serially connected, with 10 mM NaCl as eluent), and the corresponding elution curves are given in Fig. 5a. Elution curves obtained following acid hydrolysis have been published earlier [7]. The main peak in the elution profiles moves towards higher elution volumes with increasing degradation times, in accordance with the decrease in M_w. The elution was monitored by a LALLS detector and a refractive index detector, which permits the calculation of molecular weights. The on-line calculated molecular weights (Fig. 5b)

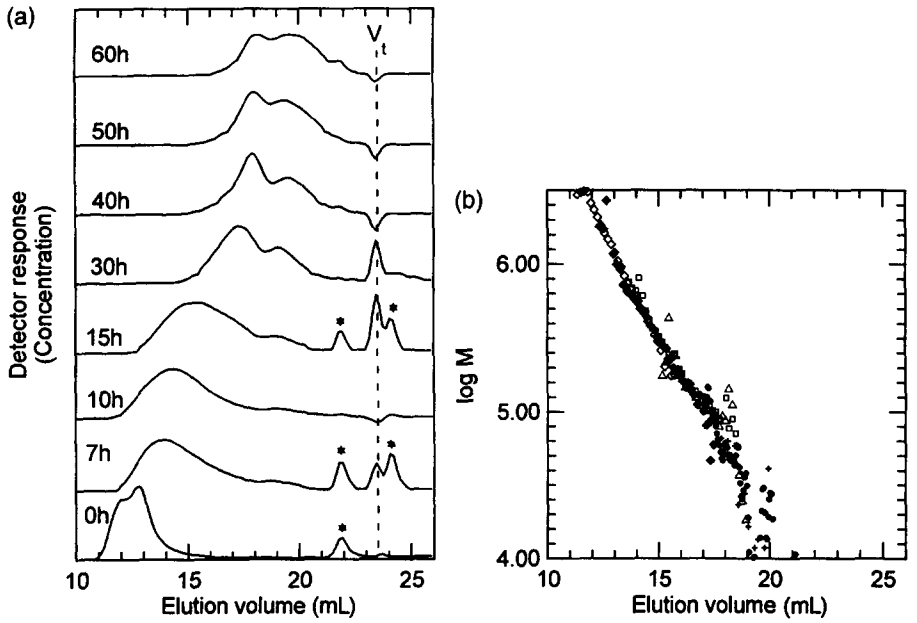

Fig. 5. Size-exclusion chromatography profiles (refractive index detector) (a) and the on-line calculated M values (b) of xanthans (degraded with H_2O_2/Fe^{2+} at 20°C). Solvent: 10 mM NaCl. Symbols and corresponding samples in (b): 4 h (◇), 15 h (◆), 25 h (□), 30 h (△), 50 h (+), and 60 h (●).

decrease with the elution volume, and although the curves cover different M-ranges they fall essentially on the same line. The amount of scattered light was too low to permit estimates of the molecular weight for elution volumes larger than 18 mL ($M < \sim 60{,}000$).

A significant finding in Fig. 5a is the appearance of a separate peak eluting at ~ 19–20 mL. The relative amount of material eluting in these peaks cannot be accurately assessed due to overlap with the main peak, but it is clearly seen that the amount increases with increasing degradation time. By extrapolation of the data in Fig. 5b the molecular weight of the material eluting in the second peak is estimated to lie in the range $10–30 \times 10^3$. These values must be regarded as rough estimates, since they may represent fragments which differ in conformation and shape from the starting material (see below). An elution volume of 20 mL corresponds to a pullulan standard with $M = 48 \times 10^3$. When the ionic strength of the eluent was increased to 0.1 M (NaCl), the elution curves of the most degraded samples ($\geq$ 15 h) shifted closer to the salt peak. The shift increased with decreasing M_w, but all elution curves retained their multimodal shape (data not shown). This indicates that the shape of the highly degraded xanthans depends on the ionic strength to a larger extent than high-molecular-weight xanthans. This is in accordance with an observed increase in chain flexibility [7], allowing for a more typical polyelectrolyte character. The same type of multimodal molecular-weight distribution was also observed earlier for xanthan degraded by acid hydrolysis [7,10], where it was shown that the second peak corresponded to conforma-

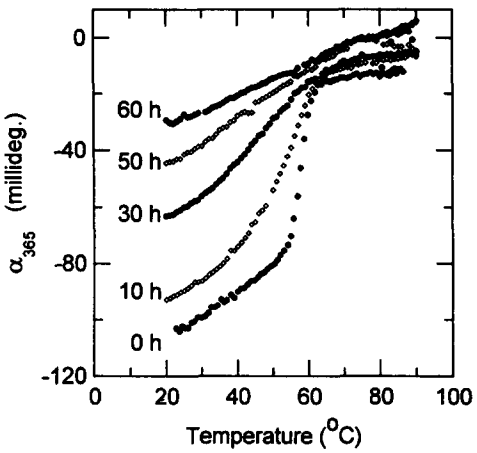

Fig. 6. Temperature dependence of the optical rotation (α_{365}) for xanthans degraded by H_2O_2/Fe^{2+} at 20°C. Solvent: 10 mM NaCl. Xanthan concentration: 1.68 mg/mL.

tionally disordered, single-stranded oligomers that had been released from the double-stranded structures. We take the data in Fig. 5a as a strong indication for the same phenomenon occurring upon degradation with H_2O_2/Fe^{2+}, i.e. a progressive release of single-stranded oligomers.

The components eluting just before and after the salt peak (marked with an asterisk in Fig. 5a) are most probably contaminants since they did not appear in two samples (10 and 40 h) that were prepared and analyzed in a separate experiment.

Conformational transition of xanthans degraded with H_2O_2/Fe^{2+}. Optical rotation studies.—Fig. 6 shows the optical rotation in 10 mM NaCl as a function of temperature for samples degraded for 0, 10, 30, 50, and 60 h. The polymer concentration was the same (1.68 mg/mL) in all cases. Due to pronounced hysteresis, only data for the first heating cycle are shown. The curves are quite similar to those obtained for partially hydrolyzed xanthans [6,7], showing the characteristic cooperative order-disorder transition near 60°C at this particular ionic strength. Two distinct features accompanies degradation with H_2O_2/Fe^{2+}. First, the optical rotation corresponding to the ordered conformation (linear region below the transition, as at 30°C) increases with increasing degradation times, whereas only a small increase is seen in the disordered conformation (as at 80°C). Secondly, the transition becomes broader with time. In order to obtain more precise information, the curves were analyzed further, as shown in Fig. 7. The linear parts of the optical rotation curves were assigned to the fully ordered state (lower line) and disordered state (upper line), recognizing that these assignments become gradually more uncertain for the most degraded samples. The fractional order (f), corresponding to the fraction of ordered residues in the glucan backbone, was then calculated as described earlier [6]. The f-data (open symbols in Fig. 7) show more clearly that the transition broadens with increasing degradation time, whereas the transition temperature (T_m, $f = 0.5$) is nearly constant or decreases slightly (observed values: 58, 55, 52, and

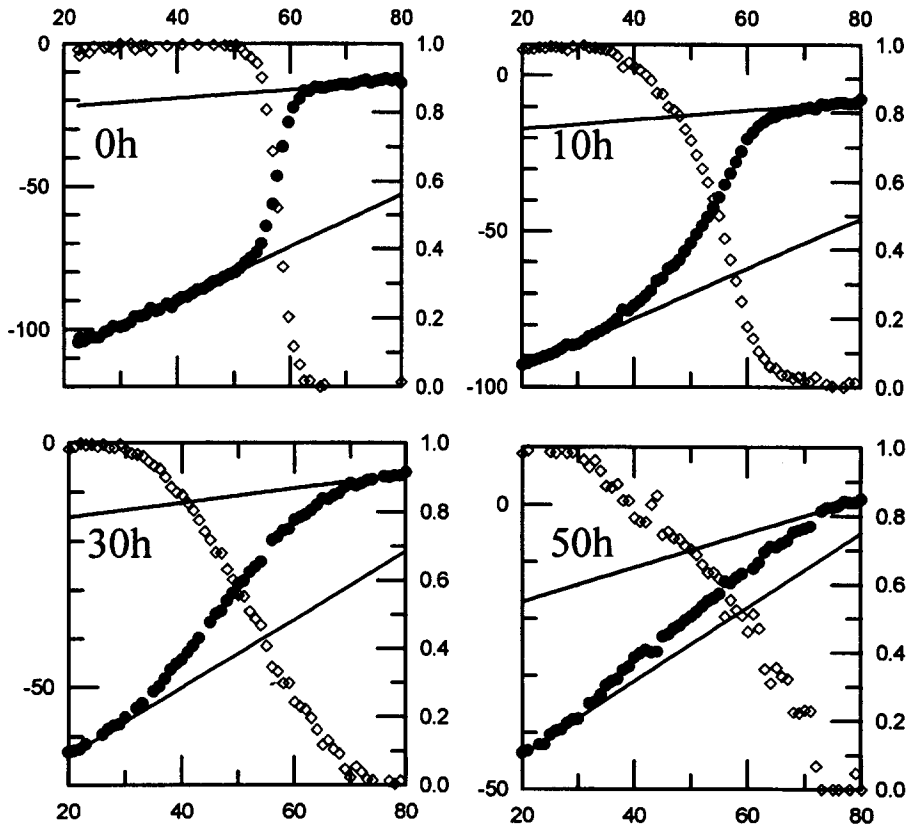

Fig. 7. Assignment of regions corresponding to the fully ordered (lower lines) and disordered (upper lines) conformations from the optical rotation data (●), and calculation of the fraction of conformationally ordered residues (◇, right *Y*-axes) for xanthan degraded by H_2O_2/Fe^{2+} at 20°C for 0, 10, 30, and 50 h. Note that different scales are used for the values of α_{365} (left *Y*-axes).

59°C for degradation times 0, 10, 30, and 50 h). The high value for the 50-h sample most probably reflects experimental uncertainty rather than a systematic trend.

4. Discussion

The degradation of double-stranded xanthan by H_2O_2/Fe^{2+} shares many of the features that are also observed by acid hydrolysis. Such features include extensive depolymerization of the glucan backbone, changes in the structure of the side chains, and the release of single-stranded oligomers. A dominating factor with respect to the physical behavior of partially degraded xanthans seems to be the molecular weight or equivalently, the degree of chain scission (α), irrespective of the type of degradation, although the influence on the chemical structure of the side chains may differ in the two cases.

Measurements of the formation of reducing ends in the glucan backbone reveal in both cases particularly interesting information regarding the depolymerization processes. For depolymerization with H_2O_2/Fe^{2+} the formation of reducing ends obeys pseudo first-order kinetics over the whole range of molecular weights, indicating that the degradation of the backbone indeed occurs in a random fashion. In contrast, the data from acid hydrolysis shows that the depolymerization rate increases with time. We suggest that the increased degradation rate is related to the release of shorter, single-stranded xanthan fragments where the glucan backbone is hydrolyzed more rapidly than in the double-stranded regions of the molecule. A possible explanation [3] for the stabilizing effect occurring in the early stages of the degradation can be inferred from the proposed reaction mechanism for acid hydrolysis [22]. The incorporation into a quite rigid double-stranded structure may lead to steric hindrance in adopting the half-chair conformation of the intermediate carbonium ion, and possibly, to an increased tendency to reversion of the reaction due to the proximity of the carbonium ion to hydroxyl groups at the newly formed non-reducing end. In contrast, the degradation with H_2O_2/Fe^{2+} is apparently not influenced by the strandedness, suggesting that glycosidic linkages are cleaved by another mechanism.

The release of the glucose monomer upon acid hydrolysis (Fig. 2) shows a very special behavior. For a truly random process, one would expect that the fraction of free glucose should equal α^2. However, this value is largely exceeded at high degradation times. A possible model for liberation of glucose, which in any case requires hydrolysis of a minimum of two linkages, is that hydrolysis of the first linkage is rate limiting, whereas the newly formed terminal glucose (reducing or non-reducing) is rapidly hydrolyzed. In this case the fraction of glucose monomer would be close to α. Moreover, the removal of side chains caused by hydrolysis of the inner mannose leads to regions devoid of side chains [3–8]. The removal of side chains in 0.1 M HCl at 80°C occurs with a pseudo first-order rate constant of 0.0025 h^{-1} (ref. [7]), that is ~ 4–12 times faster than the formation of reducing ends in the backbone. This process exposes three consecutive, unbranched glucose residues. If one of the tree linkages in such regions is first hydrolyzed (in the rate-limiting step), followed by rapid removal of the three unbranched residues, the amount of free glucose monomer would be 3α. It is obvious from Fig. 2 that neither of the proposed mechanisms adequately explain the observed values, except in the very late stages of the degradation. In fact, most ($> 80\%$) of the free glucose is liberated in the period after about 120 h, that is for $\alpha > \sim 0.05$. The major event in this interval is the release of single-stranded fragments (Fig. 5 in ref. [7]). We therefore suggest that glucose monomer is primarily liberated from the single-stranded fragments, and that the liberation of the fragments themselves is the rate-limiting step. Regions within these fragments that are devoid of side-chains may undergo further hydrolysis, and give rise to the high glucose values seen in late stages of the degradation.

In Fig. 8 are shown the measured values of M_w plotted a function of the degree of chain scission (α) for both types of degradation. The two curves lie very close to one another, suggesting that M_w is a unique function of α irrespective of the degradation type. This also suggests that all or at least most of the chain scissions induced with H_2O_2/Fe^{2+} involves the formation of a reducing end. Fig. 8 further gives the

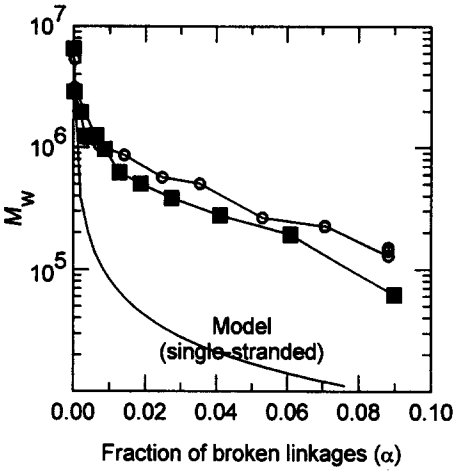

Fig. 8. Plot of M_w vs. the degree of chain scission (α) for degradation with acid hydrolysis (■) and with H_2O_2/Fe^{2+} (○). Model curve for the random depolymerization of a single-stranded polymer is included (solid line).

theoretical α-M_w relation [3] expected for the random degradation of a single-stranded polymer with $M_w = 5 \times 10^6$. The figure illustrates that the double-stranded structure retains a much higher M_w (factor of ~ 10–15) than a single-stranded polymer at the same degree of chain scission. This further suggests that only one out of 10–15 broken linkages in the glucan backbone actually gives rise to a decrease in M_w, and that the partially degraded xanthans therefore contain a high number of unexposed chain ends, as illustrated in Fig. 9. The number-average degree of polymerization (DP_n, in terms of glucose residues, corresponding to one half repeating unit) of the individual chains comprising the complex, double-stranded structure, equals $1/\alpha$. It follows for example that a sample degraded to $M_w = 2 \times 10^5$ and hence $\alpha = 0.06$ (Fig. 8) actually consists on average of 14 individual chains that form a larger double-stranded structure stabilized by non-covalent linkages. We assume [3] here that $M_n = 1/2 M_w = M_0 DP_n$, and $M_0 =$ 422 (ignoring for the sake of simplicity the reduction in the equivalent weight of the repeating unit due to degradation in the side chains). It is to our knowledge the first time that such a metastable structure (Fig. 9) has been observed among the polysaccharides, whereas it is known that similar structures can exist in DNA [9]. It follows that other multiple-stranded polysaccharides, as in triple-stranded scleroglucan or schizophyllan, may be partially degraded to form corresponding structures, but this topic remains to be further explored.

Degradation of xanthan with H_2O_2/Fe^{2+} leads to a reduction in the Man/Glc ratio while the Man/GlcA ratio remains essentially constant (within experimental error). This is most easily explained by a mechanism where the entire side chain is split off. This suggests that the region near the glycosidic linkage between the α-D-mannose and the glucan backbone is attacked, presumably [1,23] by the hydroxyl radical formed through the Fe^{2+}-catalyzed decomposition of H_2O_2 [24]. The secondary reactions which eventu-

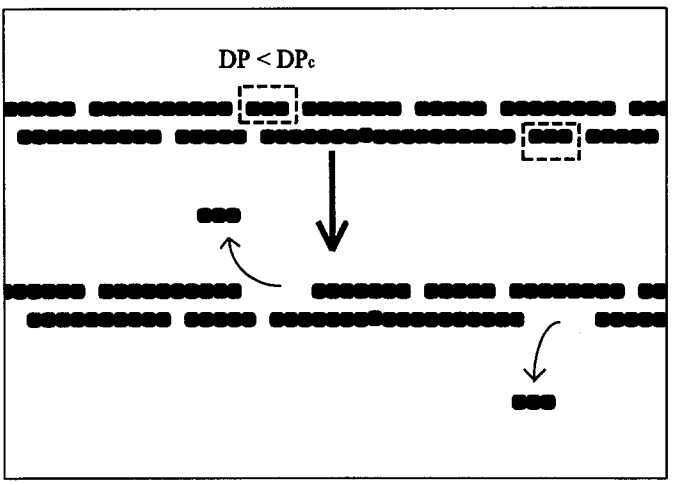

Fig. 9. Schematic representation of a partially degraded xanthan containing shorter chains stabilized within the double-stranded structure and the release of oligomers that are too short to allow their incorporation in the duplex. Note that side chains are omitted in the figure, and that each drawn unit may consist of several backbone residues.

ally lead to cleavage of the linkage cannot be inferred from the present observations. This degradation pattern deviates from that obtained by acid hydrolysis, since the latter preferentially removes the terminal β-D-mannose [3–8]. Systematic studies of partially hydrolyzed xanthans showed [5] that the content of both β-D-mannose to a large degree determined the magnitude of conformation-linked parameters such as the optical rotation, circular dichroism, and transition enthalpy, although the transition temperature was independent of its content. Also in the case of degradation with H_2O_2/Fe^{2+} an influence on the optical rotation was observed (Fig. 6). Below T_m (as at 30°C) an increase in α_{365} was observed with increasing degradation times, whereas the influence of the degradation time on α_{365} was very small above T_m (as at 80°C). The increase in α_{365} below T_m can in part be explained [6] by the removal of side chains, which contribute significantly to the magnitude of α_{365} in addition to the increase in α_{365} due to an increase in the fraction of conformationally disordered residues. However, for the 60-h sample, where a conformational transition could hardly be detected, ~ 60% of the side chains were still present (data in Fig. 4 extrapolated to 60 h), suggesting that other factors also contribute. The obvious possibility is then that the fraction of conformationally disordered residues increases as a result of the degradation. This is supported by the gradual release of low M_w fragments (the second peak in the SEC chromatograms) which are assumed to be conformationally disordered [7]. After 60 h of degradation it seems that the relative amount of such fragments is roughly in the order of 50%, which then could account for half of the increase in α_{365} below T_m, whereas the remaining increase is tentatively attributed to the removal of side-chains. Although T_m appeared to be independent of M_w, a broadening of the transition was observed with decreasing M_w. This contrasts with the observations made for acid hydrolysis, which did not result

in the same extent of broadening [6,7]. Such broadening is generally expected for cooperative transitions of this type due to the effect of chain length on the cooperativity. The difference between the two degradation types may well be associated with different degradation patterns in the side chains.

As also shown previously for acid hydrolysis [7,10], prolonged degradation of xanthan with H_2O_2/Fe^{2+} results in the release of conformationally disordered fragments which appear at higher elution volumes in the size-exclusion chromatography experiments (Fig. 5a). The shift towards a multimodal molecular-weight distribution (Fig. 5a) with increasing degradation time can be explained by the mechanism depicted in Fig. 9 [5,7]. The central feature is that the DP of some of the oligomers is below the critical value (DP_c) which is needed to allow the cooperative stabilization within a duplex structure. The enthalpy gain associated with the formation of non-covalent linkages between the chain segments, which is proportional to DP, will for short fragments not be large enough to compensate for the entropy loss associated with duplex formation. The value of DP_c is of fundamental interest although it is expected to depend strongly on parameters such as temperature and ionic strength. Estimation of DP_c applies therefore only to the experimental conditions where analysis of the degradation takes place. From the relationship between elution volume and M_w in the SEC analysis (Figs 5a and 5b) we may roughly estimate DP_c. The second peak in the chromatograms, which is attributed to the released fragments, corresponds according to Fig. 5b to a M_w in the range of $10^{4.2} = \sim 16{,}000$. However, this average value will be an underestimation, since further depolymerization of these fragments occurs during the experiments. We have previously [7] estimated DP_c to a value corresponding to 10–15 glucose residues based on the relative content of low molecular weight fragments (C_{single}/C_{total}) by means of a Monte Carlo model [5]. The problem of further degradation of the fragments is then circumvented, but requires that C_{single} can be estimated with reasonable accuracy. Unfortunately, there is too much overlap between the peaks to allow good estimates of the areas, and this approach was therefore not carried further.

The accelerated degradation of polysaccharides by H_2O_2/Fe^{2+} to mimic naturally occurring ORD reactions has several advantages over methods like acid hydrolysis, particularly in questions regarding conformational effects. First, it may be assumed that the nature and specificity of the H_2O_2/Fe^{2+} induced degradation are more representative than acid hydrolysis. A second feature is that although acid hydrolysis cleaves glycosidic linkages by well understood mechanisms it also stabilizes xanthan by inducing the ordered conformation (increasing T_m). For instance, at 80°C and low ionic strength xanthan is more rapidly degraded at pH 4 than at pH 2 [3], and high temperatures are necessary to achieve reasonably rapid degradations. High temperatures also limit the range of physical methods that can be used to monitor the degradation, unless the samples are cooled, a step which may influence the degree of conformational order. In contrast, degradation with H_2O_2/Fe^{2+} proceeds rapidly at ambient temperature, and the conformational state can, in principle, be varied more independently of the degradation agent. However, in contrast to H^+, H_2O_2 is consumed in the reaction with Fe^{2+}, and leads to a decrease in the rate of polymer degradation with time.

In conclusion, degradation of double-stranded xanthan with H_2O_2/Fe^{2+} proceeds in a manner which lies close to that observed earlier [3–8] for acid hydrolysis. Some

differences regarding changes in the side-chains are observed, but the effects ascribed to the double-stranded state largely governs the stability properties.

Acknowledgements

This work was partially financed by the Research Council of Norway (grant BT27487) and Statoil (VISTA-grant V6314).

References

[1] A. Herp, in W. Pigman and D. Horton (Eds.) *The Carbohydrates*, Vol. Ib, Academic Press, New York, 1980, pp 1276–1287.
[2] W. Littmann, W. Kleinitz, B.E. Christensen, B.T. Stokke, and T. Haugvallstad, *Soc. Petrol. Eng. J.*, (1992) paper 24120.
[3] B.E. Christensen and O. Smidsrød, *Carbohydr. Res.*, 214 (1991) 55–69.
[4] T. Hjerde, T.S. Kristiansen, B.T. Stokke, O. Smidsrød, and B.E. Christensen, *Carbohydr. Polym.*, 24 (1994) 265–275.
[5] B.T. Stokke, B.E. Christensen, and O. Smidsrød, *Macromolecules*, 25 (1992) 2209–2214.
[6] B.E. Christensen, K.D. Knudsen, O. Smidsrød, S. Kitamura, and K. Takeo, *Biopolymers*, 33 (1993) 151–161.
[7] B.E. Christensen, O. Smidsrød, A. Elgsaeter, and B.T. Stokke, *Macromolecules*, 26 (1993) 6111–6120.
[8] B.E. Christensen, O. Smidsrød, and B.T. Stokke, in M. Yalpani (Ed.), *Carbohydrates and Carbohydrate Polymers. Analysis, Biotechnology, Modification, Antiviral, Biomedical and Other Applications*, ATL Press, Mount Prospect, 1993, pp 166–173.
[9] C.A. Thomas, *J. Am. Chem. Soc.*, 78 (1956) 1861–1868.
[10] B.T. Stokke and B.E. Christensen, *Food Hydrocolloids*, (1995) in press.
[11] H. Uchiyama, Y. Dobashi, K. Ohkouchi, and K. Nagasawa, *J. Biol. Chem.*, 14 (1990) 7753–7759.
[12] O. Smidsrød, A. Haug, and B. Larsen, *Acta Chem. Scand.*, 17 (1963) 2628–2637.
[13] F. Lambert and M. Rinaudo, *Polymer*, 26 (1985) 1549–1553.
[14] B.T. Stokke, P. Foss, B.E. Christensen, C. Kierulf, and I.W. Sutherland, *Int. J. Biol. Macromol.*, 11 (1989) 137–144.
[15] C. Kierulf and I.W. Sutherland, *Carbohydr. Polym.*, 9 (1988) 185–194.
[16] P. Foss, B.T. Stokke, and O. Smidsrød, *Carbohydr. Polym.*, 7 (1987) 421–433.
[17] M. Rinaudo, M. Milas, F. Lambert and M. Vincendon, *Macromolecules*, 16 (1983) 816–819.
[18] F. Callet, M. Milas and M. Rinaudo, *Int. J. Biol. Macromol.*, 9 (1987) 291–293.
[19] N.W.H. Cheetham and E.N.M. Mashimba, *Carbohydr. Polym.*, 17 (1992) 127–136.
[20] S.L. Wellington, *Soc. Pet. Eng. J. Des*, (1983) 901–912.
[21] J.E. Hodge and B.T. Hofreiter, *Methods Carbohydr. Chem.*, 1 (1962) 386–388.
[22] J.N BeMiller, *Adv. Carbohydr. Chem.*, 22 (1976) 25–108.
[23] O. Smidsrød, A. Haug, and B. Larsen, *Acta Chem. Scand.*, 19 (1965) 143–152.
[24] J. Weiss, *Adv. Catal.*, 4 (1952) 343–365.